

# Effect of Eleven Years in Earth Orbit on a Mirror Surface

Michael J. Mirtich,\* Herman Mark,† and William R. Kerslake‡  
NASA Lewis Research Center, Cleveland, Ohio

At NASA Lewis Research Center, micrometeoroid impact was simulated by accelerating micron-size particles to hypervelocities. Any changes in the optical properties of surfaces exposed to this impact were then evaluated. The degradation of optical properties of polished metals and thin metallic films after exposure to this environment was determined as a function of impacting kinetic energy/area. A calibrated sensor, 2000 Å Al/stainless steel, was developed to detect the micrometeoroid environment and to evaluate the degradation of the optical properties of thin aluminum films in space. This sensor was flown on OSO III and SERT II, satellites that were launched in 1967 and 1970, respectively. No changes in the optical properties of the highly reflective surface were measured during 11 years in space. The results, as determined by the accuracy of the sensor, indicate that highly reflective surfaces should lose less than 1% of their specular reflectance in near-Earth orbit during 11 years.

## Nomenclature

$E_{cr}$	= cratering energy density, erg/cm <sup>3</sup>
$I_{BB}$	= spectral energy distribution of 420 K (756°R) blackbody
$I_{HR}$	= intensity from blackbody cavity
$M_p$	= mass of impacting particle
$T_b$	= body temperature
$T_{1,2}$	= disk temperature
$V_p$	= particle velocity
$\alpha_{sn}$	= normal solar absorptance
$\epsilon$	= exposure, $\Sigma_i \frac{1}{2} m_{pi} v_i^2$ , J
$\epsilon_{th}$	= total hemispheric emittance
$\theta_s$	= sun angle
$\lambda$	= wavelength of radiation, $\mu$
$\bar{\rho}$	= average reflectance
$\bar{\rho}_{H-A}$	= hemispheric-angular reflectance
$\bar{\rho}_{H-H}$	= hemispheric-hemispheric reflectance
$\sigma$	= Stefan-Boltzmann constant, $= 1.713 \times 10^{-9}$ Btu/h ft <sup>2</sup> °R <sup>4</sup>
$\phi$	= intensity of incident radiation

## Subscripts

$a$	= after exposure to $\epsilon$
$i$	= initial value
$L$	= laboratory conditions
$SP_1$	= space conditions 1
$\infty$	= infinite exposure to particle impaction

## Introduction

**A** RESURGENCE of interest in placing large solar concentrator solar dynamic systems in space for power generation has renewed interest in maintaining the integrity of the

optical properties of highly specular reflecting surfaces in the near-Earth space environment. One of the hazards of concern needing evaluation is the micrometeoroid environment. It has been shown that highly reflective polished metals and thin-film coatings degrade when exposed to simulated micrometeoroids.<sup>1</sup> At NASA Lewis Research Center, a shock tube was used to simulate the phenomenon of micrometeoroid impact by accelerating micron-size particles to hypervelocities. The optical properties of surfaces exposed to this impact were then evaluated using a Hohlraum reflectometer and a space environment facility. Thus, the degradation of the optical properties of polished metals and thin metallic films after exposure to simulated micrometeoroids was determined as a function of impacting kinetic energy per area. From this work, a calibrated mirror surface sensor (2000 Å Al/stainless steel) was developed that could not only detect the micrometeoroid environment but also evaluate the degradation of the optical properties of the thin aluminum film in space. This mirror surface sensor was flown on the OSO (Orbiting Solar Observatory) III and SERT (Solar Electric Rocket Test) II Earth-orbiting satellites that were launched in 1967 and 1970, respectively. Data were obtained for as long as 11 years in orbit on the SERT II.

When the sensor was placed on these satellites (mid to late 1960's), there was a lack of resolution in the measured flux of micrometeoroids near the Earth (from 0.02 to several Earth radii).<sup>2,3</sup> Reference 2 contains 48 papers on the micrometeoroid environment. These data are plotted from the direct measurements of interplanetary dust as recorded by various sensors on board a variety of satellites (Fig. 1). This is a cumulative micrometeoroid flux (a sensor capable of measuring a  $10^{-10}$ -g particle counts all particles  $10^{-10}$  g or greater), which seems to indicate that there are few or no micrometeoroid particles smaller than  $10^{-12}$  or  $10^{-13}$  g. For larger-size meteoroid particles, either photographically or optically visible ( $10^{-5}$  g), efforts to measure the flux have succeeded in obtaining a satisfactory picture of the situation, at least from the engineering and even, perhaps, from the scientific point of view. However, for the fluxes of smaller particles that may exist in near-Earth space, these flight experiments produced seemingly believable data that differed by four to five orders of magnitude.<sup>2,3</sup> This unsatisfactory situation existed for many reasons.

The list of transducers used for measuring the flux of particles in the range of interest ( $10^{-8}$  to  $10^{-14}$  g) is almost endless.<sup>2,3</sup> One difficulty with all of the detectors is the problem of separation of spurious signals from those actually

Presented as Paper 88-0026 at the AIAA 26th Aerospace Sciences Meeting, Reno, NV, Jan. 11-15, 1988; received Aug. 13, 1988; revision received March 16, 1989. Copyright © 1989 American Institute of Aeronautics and Astronautics, Inc. No copyright is asserted in the United States under Title 17, U.S. Code. The U.S. Government has a royalty-free license to exercise all rights under the copyright claimed herein for Governmental purposes. All other rights are reserved by the copyright owner.

\*Senior Research Scientist, Space Power Division. Member AIAA.

†Retired; formerly, Deputy Director, Office of Research and Technology Assessment. Associate Fellow AIAA.

‡Retired; formerly, Member of Space Propulsion Division. Associate Fellow AIAA.

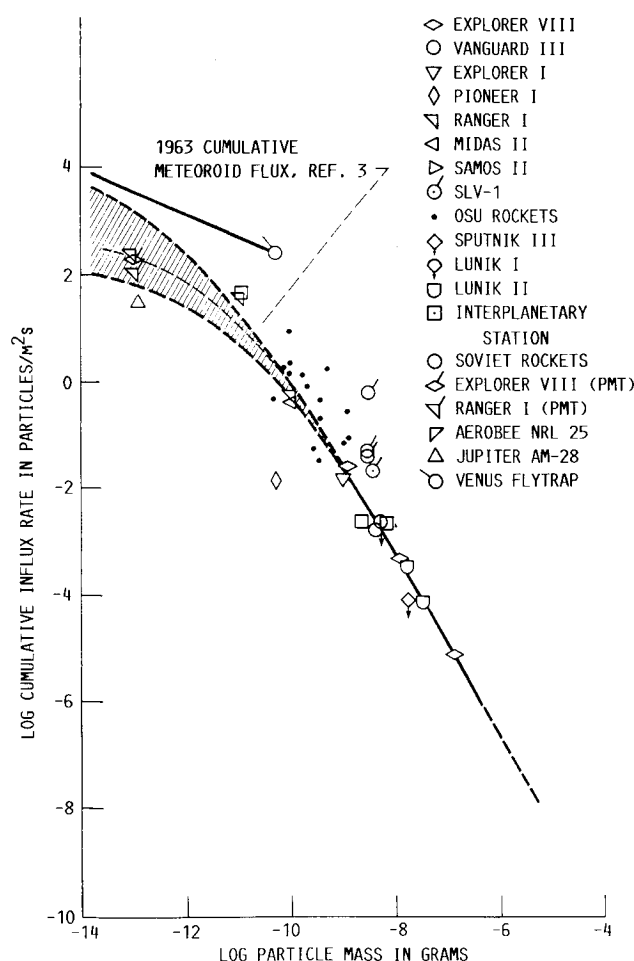


Fig. 1 Cumulative micrometeoroid flux based on direct measurements of interplanetary dust, 1963.

caused by particle impact. Each of the aforementioned transducers had a number of possible sources of spurious signals. Consequently, many of the measurements could have included such an abundance of spurious signals that the results differed by four to five orders of magnitude (see Fig. 1 for a  $10^{-10}$ -g particle).

The thermal behavior of polished metal and thin film surfaces exposed to a simulated micrometeoroid flux is presented in Ref. 4. These two studies show that relatively large changes in surface optical properties (emittance and solar absorptance) can be affected by erosion caused by simulated micrometeoroid exposure. It follows, therefore, that the erosion of surface optical properties in a flight experiment might be an excellent way of determining the rate of meteoroid flux in the  $10^{-8}$  to  $10^{-12}$ -g range by determining the effects of this flux on surface optical properties, an engineering problem of importance.

Surfaces in space and their optical properties can also be degraded by other features of the environment and by micrometeoroid erosion. Atomic oxygen, ultraviolet radiation, and proton and electron bombardment also rapidly degrade many surfaces.<sup>5-7</sup> Thus a transducer surface had to be chosen whose optical properties would be affected only by micrometeoroid erosion and by nothing else in the environment.<sup>4,6</sup> Polished metal surfaces seemed a perfect choice. Not only are they relatively impervious to radiation damage, but their surface properties are rapidly degraded by erosive micrometeoroid bombardment. However, problems that can arise from their use as transducers are of a different nature. Because of their extremely low absorptance and emittance, polished metal surfaces are ideally suited for the detection of

small amounts of surface damage, but these very low-valued optical properties can cause difficulties in properly isolating samples of these materials from the effects of energy exchange with the orbiting vehicle.

This problem was resolved in ground studies simulating exposure to micrometeoroid erosion and the effect of such erosion on orbital temperature histories.<sup>1,7,8</sup> It was now possible to run a ground-flight experiment involving measurement methods based on the 1963 micrometeoroid flux model (the only model available at that time), which could determine the erosive micrometeoroid flux in orbit as well as its effect on critical surfaces. Results of these space experiments (ground micrometeoroid simulation and sensor calibration using a large solar-space-environment simulation chamber) and conclusions regarding the (1987) micrometeoroid and debris flux models are presented in this paper.

### Ground Calibration

As a result of a program at NASA Lewis in the 1960's in which polished metal surfaces were exposed to impactation by high-speed, micron-size particles in the laboratory, a quantitative relation between exposure energy and the degradation of the surface optical properties was found.<sup>1</sup> It became apparent that a flight experiment could be used to monitor surface optical properties (i.e., reflectance) to determine exposure to micrometeoroid flux. It was determined by Mark et al.<sup>4</sup> that reflectance measurements in flight without a reflectometer are possible and can be made with thermal measurements only. In Ref. 4, a simulated micrometeoroid exposure-temperature calibration was made in ground studies on several polished metal and thin-film metal surfaces. Some background information on micrometeoroid simulation and the method of micrometeoroid exposure-temperature calibration are presented in this section.

### Simulation of Micrometeoroid Exposure

In spite of the fact that the maximum attainable speeds to which particles could be accelerated intact in ground-simulation tests were only a fraction of the speeds of micrometeoroid particles in Earth orbit, it was believed that the phenomenon of hypervelocity impactation with micrometeoroids could be simulated adequately by impactation with particles at attainable speeds. In order to obtain a calibration of micrometeoroid exposure against equilibrium temperature of a thermally isolated disk under space conditions, a means of characterizing exposure both on the ground and in space was needed. Laboratory exposure quantities and change in surface property (reflectance, for instance) due to exposure are known for laboratory simulation of micrometeoroids. However, in space a change in surface property could have been caused in a number of ways, and thus, not having a unique tie to the environment that caused it, fails to characterize this environment as well as the exposure itself. Therefore, the actual physical quantity to use for measuring the exposure is in question. Since a number of earlier experimental and theoretical investigations have indicated that the volume of craters formed in targets as a result of impactation with high-speed projectiles is proportional to the kinetic energy of the projectiles, the sum of the kinetic energies of the particles striking the surface up to any time was chosen as the physical quantity characterizing the exposure. The analysis that follows is presented in Refs. 1 and 9 and provides a useful relation connecting the surface reflectance with the exposure characterized by the kinetic energy of the impacting particles. From Ref. 1, the expression for reflectance  $\bar{\rho}_a$  of a metal surface of area  $A_o$  exposed to impactation by particles having a total kinetic energy  $\epsilon$  in joules is

$$\bar{\rho}_a = \bar{\rho}_i \left[ 1 - \left( 1 - \frac{\bar{\rho}_\infty}{\bar{\rho}_i} \right) (1 - e^{-K\epsilon}) \right] \quad (1)$$

where

$$K = \left( \frac{2}{A_o} \right) \left( \frac{3\pi^{1/2}}{4E_{cr}} \right)^{2/3} (M_p V_p^2)^{-1/2} \quad (2)$$

Equations (1) and (2) allow an analytical extrapolation from the measured total energy required for a given laboratory-caused surface optical property change to the total energy required in space for the same surface optical property change. This extrapolation requires evaluating  $K$  for space and can be done if the kinetic energy of the particle in space causing most of the surface damage can be estimated reasonably.

The experimental procedure for producing the laboratory damage to the surfaces is described in detail<sup>1</sup> but will only be discussed briefly in the following paragraphs. First, polished surfaces of soft aluminum, stainless steel, and stainless steel coated with 1900 Å of aluminum were bombarded by clouds of SiC particles having an average diameter of 6 μm and a speed of 2.6 km/s. The particles were accelerated by the aerodynamic drag of the short-duration flows in a shock tube, and the resultant kinetic energies

$$\epsilon = \sum_i \frac{1}{2} M_{pi} V_{pi}^2 \quad (3)$$

were obtained from strip-film camera measurements for particle speed and microbalance collection measurements to determine the total number of particles striking a given area.<sup>1</sup> The measurement of speed and number of particles striking a plate were quite accurately reproducible. The laboratory exposure energies were measured and are presented in J/cm<sup>2</sup>. In each series (for each target material), the disks, 4.45 cm<sup>2</sup>, were exposed nominally to 0, 1, 2, 4, and 6 J (0, 0.22, 0.44, 0.89, and 1.35 J/cm<sup>2</sup>). This range of exposures represents changes in the reflectance of a single disk from its original value near 1.0 to about 0.5.

Thus, there is the possibility of quantitatively exposing surfaces in the laboratory to impaction by high-speed particles of known energy per unit area and measuring the damage by means of a change of reflectance and then predicting [Eqs. (1) and (2)] the equivalent space exposure in energy per unit area required to produce the same surface damage. Having the exposure-surface damage relation and the surface damage-equilibrium temperature relation obtained in the simulated space environment (described in a later section) allows the design of a space experiment in which the simple monitoring of temperature of a disk in space determines not only surface damage but also the actual micrometeoroid exposure causing the damage as a function of time. This follows, of course, only if it is assumed that micrometeoroid exposure is causing the surface damage. It also is necessary to assume that normal impingement is sufficient to simulate impingement from all directions. This is shown to be so and is discussed in Ref. 10.

#### Determination of Surface Optical Properties

The disks used in this study, chosen from their good reflective properties, were made of stainless steel, aluminum, and a stainless-steel substrate with a vapor-deposited coating of aluminum, 1900 Å thick. This coating is sufficiently thick for the surface to exhibit the optical properties of aluminum as long as the coating remains undamaged.

The disks were chosen 2.38 cm in diameter and 0.046–0.16-cm thick because these are appropriate dimensions for a sample in the heated-cavity spectrometer system for making reflectance measurements. In this system, a Perkin-Elmer 13U spectrometer compares, in a given wavelength band, radiation from a blackbody cavity at about 870 K to the total radiation reflected from a water-cooled sample in the same wavelength band. This technique works well in the infrared region, but is not satisfactory at shorter wavelengths because of insufficient radiation from the heated cavity below

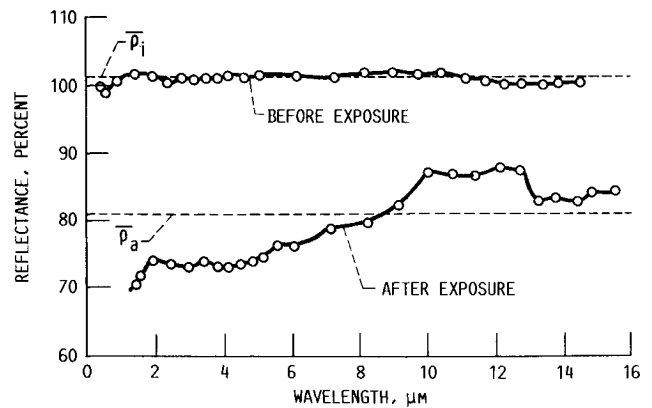


Fig. 2 Spectral reflectance  $\bar{\rho}_{H-A}$  for 1900 Å aluminum on stainless steel substrate exposed to approximately 0.2 J/cm<sup>2</sup> of hypervelocity impaction.

a wavelength of about 1 μm. The intensity ratios obtained ( $I_{REFL}/I_{HR}$ ) are plotted as a function of wavelength and are presented for 1900 Å Al on stainless steel in Fig. 2, both before and after exposure to impaction with approximately 0.22 J/cm<sup>2</sup> of 6-μm-diam SiC particles traveling at 2.6 km/s. The average values of these spectral data are presented also. The average reflectance is defined here as the single value that will reflect the same amount of energy arriving from a 420 K (756°R) blackbody source as does the sample, i.e., the average reflectance  $\bar{\rho}_a$  is given by

$$\bar{\rho}_a = \int_{\lambda_1}^{\lambda_2} \rho_{H-A}(\lambda) I_{BB}(\lambda) d\lambda / \int_{\lambda_1}^{\lambda_2} I_{BB}(\lambda) d\lambda \quad (4)$$

where

$$\rho_{H-A} = \frac{I_{REFL}}{I_{HR}}, \quad \lambda_1 = 1.5 \mu\text{m}, \quad \lambda_2 = 15.5 \mu\text{m}$$

The normal solar absorptance was determined from measurements made in the space environment simulator during transient heating of the exposed disks mounted in a simulated space vehicle. The total hemispheric emittance of the disks was obtained during transient cooling. Comparisons were made later between equilibrium temperatures calculated from the values of thermal optical properties obtained by these transient experiments and the actual equilibrium temperatures attained by the disks in a solar simulator.<sup>4</sup> Infrared reflectances are also compared with thermally obtained disk emittances. The space chamber thermal experiment<sup>4</sup> will be briefly outlined later in this paper.

#### Simulated Exposure and Surface Damage

Reflectances for all the disks were obtained both before and after exposure, and spectral reflectance data of the type presented in Fig. 2 were calculated from Eq. (4) to obtain average reflectance values weighted for the energy distribution corresponding to a 420 K blackbody. In Fig. 3, all of the average reflectance ratios for stainless steel, aluminum, and a aluminum on stainless steel are plotted against the total energy of the impacting particles. For an equivalent reduction in reflectance in space, we also have presented the required space exposure on two additional abscissas (see Appendix A of Ref. 4). The first is for a space particle of  $3 \times 10^{-11}$  g (a mass of one-tenth of the laboratory particle) and a speed of 10.3 km/s (compared with 2.6 km/s for the laboratory speed). The second extra abscissa is also for a  $3 \times 10^{-11}$ -g particle but at 26 km/s. In the first case, an exposure of  $\epsilon_{SP1} - 1.7\epsilon_L$  is required. In the second case,  $\epsilon_{SP2} = 2.15\epsilon_L$  is the required exposure. This increase in exposure for space conditions to obtain equivalent damage is due to the negative one-third exponential depen-

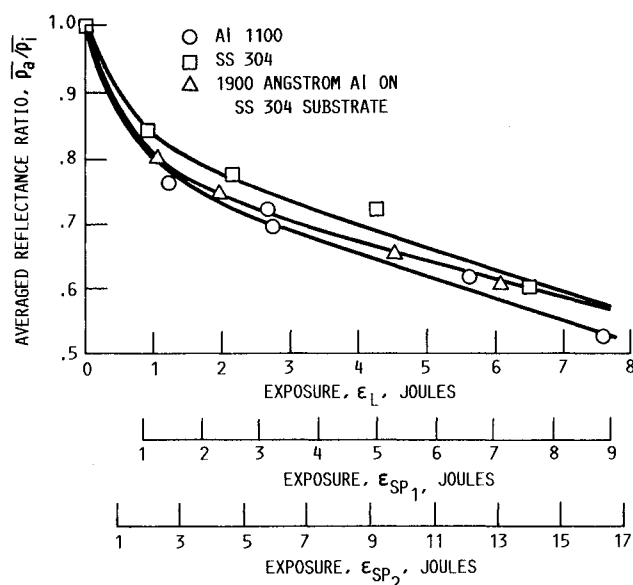


Fig. 3 Degradation of average reflectance of various metal surfaces after exposure to impact by 6- $\mu$ m SiC particles traveling at 8500 ft/s in the laboratory. (Extra abscissas added to indicate exposure necessary for equal damage in space.)

dependency on the single-particle kinetic energy of the  $K$  in Eqs. (1) and (2). Thus, as the single-particle kinetic energy increases,  $K$  decreases [Eq. (2)], and the surface damage at a given total energy of exposure is reduced (i.e., the reflectances do not fall as rapidly with total exposure).

The data in Fig. 3 indicate that the reduction in the infrared reflectance ratio of aluminum is somewhat greater at any exposure than that of stainless steel. The reflectance of both, however, falls to less than 60% of the original value after only 7.5 J (1.65 J/cm<sup>2</sup>) of laboratory exposure.

The reflectance ratio of the disk of stainless steel coated with 1900 Å of aluminum follows the reflectance ratio of aluminum until the exposures are increased to cause a 60% reduction in reflectance ratio after which the aluminum-coated stainless steel approaches that of the substrate stainless steel as the aluminum coating is being eroded away. To obtain these curves, the values for  $\bar{\rho}_\infty$ , the reflectances of the samples at infinite exposure, were determined in Ref. 11. The value for aluminum obtained at 5.6-J/cm<sup>2</sup> exposure is 0.3055. For stainless steel,  $\bar{\rho}_\infty = 0.350$  (obtained at 6.7-J/cm<sup>2</sup> exposure). In addition to pointing out the reduction in exposed surface reflectivity, Fig. 3 also suggests that the aluminum-coated disk should degrade like aluminum at first, then, after some exposure (as the coating is removed), resemble the degradation rate of the substrate stainless steel. Since the reflectance ratio degradation rate for the aluminum-coated surface has slowed to that of the stainless steel, the effect of the aluminum coating on stainless steel is to keep the absolute reflectance up throughout the experiment. That is, the reflectance remains high longer than that of aluminum alone and, hence, for a longer time than might be expected in space.

#### Space Simulation Chamber

A space environment simulation facility was used to determine the equilibrium temperature of the surfaces described in this paper.<sup>4</sup> In the working section of the inner "space" chamber, which was 1.82 m in diameter and approximately 3 m high, four characteristics of the space environment were reproduced simultaneously and as accurately as possible. The first was the low pressure of gases in space, estimated to be about  $10^{-14}$  mm Hg.

This low pressure was obtained by keeping the entire chamber wall at liquid helium temperatures by jacketing. The

liquid-helium-cooled jacket provided nearly perfect absorption capability of the space background for gases. The inner space chamber walls jacketing also produced the extremely low background temperature of space (about 4 K), thus removing any superfluous radiation source. The most important radiant energy source in space is, of course, the sun. In this facility, the radiation arriving from the sun, at Earth distance from the sun (but outside Earth atmosphere), was provided by a carbon arc lamp at the proper intensity, uniformity, and collimation angle. The resulting spectral energy distribution approximated that of the sun over the wavelength range from 0.35 to about 2.5  $\mu$ m. Details concerning the monitoring and maintenance of these conditions are presented in Refs. 4 and 12.

#### Space-Chamber-Temperature Experiment

Five identical 2.38-cm-diam (15/16-in.) polished disks were selected for a given material, and each disk was then subjected to a given amount of laboratory exposure. The exposure was increased from disk to disk. Each series of disks of a given material was then mounted on a simulated spacecraft that had been designed to minimize heat transfer between the spacecraft and the mounted disks. This was accomplished by mounting the disks on nonconducting plastic stems and shielding the back of the disks with highly reflecting cups, thus allowing a heat balance for the disks only involving received and emitted radiation from the front exposed side of the disk and a minimum loss from the unexposed side ( $8.3 \times 10^{-8}$  W/K<sup>4</sup>). The simulated vehicle was mounted in the space-environment tank so that the front faces of the disks received direct solar radiation from a direction normal to their surfaces. The front surfaces of the disks were also exposed to the cold sink of space over nearly the entire  $2\pi$  solid angle (except for the sun). Thus, the disks could arrive at the equilibrium temperature based on the heat balance between the normal energy (solar radiation) absorbed and the total hemispheric energy emitted by the front face (plus the energy loss to the supporting spacecraft structure). The equilibrium temperature for each disk was measured by a copper-constantan thermocouple embedded in the disk one-half radius out from the mounting pin at the center. The equilibrium temperature of the disk was determined by taking measurements of temperature while approaching equilibrium conditions from above and below the equilibrium temperature. During the experiment, radiation intensity was monitored by six silicon solar cells previously calibrated against a Schwarz total radiation intensity meter. The resulting variation in the equilibrium temperatures for all the disks is the result of reproducible changes in surface optical properties caused by calibrated exposure to high-speed, micron-size particle impactation. Transient temperatures were measured similarly during heating and cooling of the disks for the purpose of determining  $\alpha_{sn}$  and  $\epsilon_{th}$  by an essentially independent experiment (independent from the equilibrium experiment).

#### Results of Space-Chamber-Temperature Experiment

The major results of the temperature-equilibrium experiment are presented in Fig. 4 (tabular data are shown in Ref. 4). The "history" of the equilibrium temperature for disks of three different materials mounted on a simulated space vehicle and "flown" in a simulated space environment at 1.25 solar constant can be found in Fig. 4. These equilibrium temperatures are shown as they vary with exposure to the simulated micrometeoroid environment, the exposure being expressed in J/cm<sup>2</sup> of energy of the impacting hypervelocity particles on the 2.38-cm-diam disks. Perhaps the most important feature of these curves is that, in spite of the large exposure to impacting particles, the resulting change in optical properties measured in the laboratory, and the efforts made to isolate the disk thermally from its support, the total variation in equilibrium temperature of the disks is small but measurable. For the aluminum disk, the measured change in

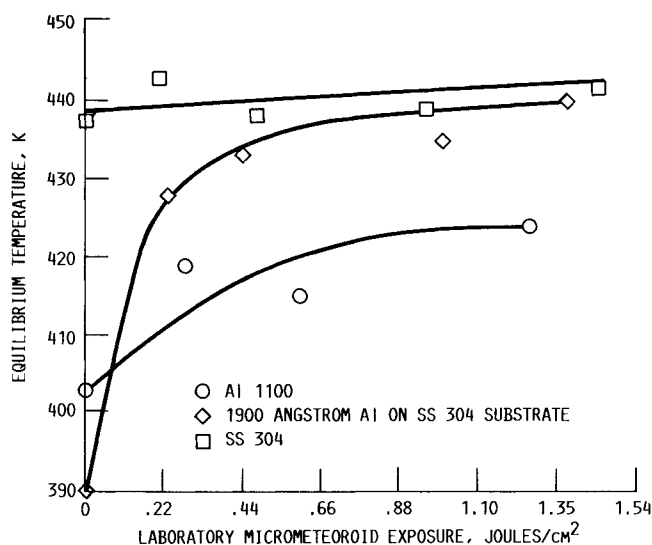


Fig. 4 Equilibrium temperature as a function of exposure to simulated micrometeoroids.

equilibrium temperature is approximately 21 K, or about 5% in absolute temperature level. For stainless steel, the temperature is almost constant, varying only about 0.1% in absolute temperature level. The largest variation occurred with the aluminum-coated stainless-steel disk, which rose 50 K due to the exposure, or about 12% in absolute temperature level.

From the information presented in Table 2 of Ref. 4, the  $\epsilon_{th}$  of Table 1 of Ref. 4 was used to calculate a reflectance (i.e.,  $\bar{\rho} = 1 - \epsilon_{th}$ ) solely for comparison with  $\bar{\rho}_a$ , the average reflectance of the disks measured by the spectrometer method. These two "reflectances" can be compared, because  $\bar{\rho}_a$  is equal approximately to  $\rho_{H-A}$  for the materials in this experiment, and  $\rho_{H-H}$  can be taken equal to  $(1 - \epsilon_{th})$  at the same temperature.<sup>4</sup> The comparisons of these two quantities for the disks are amazingly close, considering the difference in the paths traveled to obtain them. Whether or not such a comparison is strictly correct, the optical or thermal changes in surface property are certainly varying in a very similar manner with simulated exposure to the micrometeoroid environment. This similarity in the variation of reflectance with exposure, as measured by either method, suggested the possibility of making reflectance measurements in space without a reflectometer and using these reflectance measurements to determine micrometeoroid flux. This could be done by calibrating the change in temperature of a disk in a space-environment simulation chamber with the measured (elsewhere) optical change of the surface caused by calibrated exposure of the disk to the simulated micrometeoroid flux. Telemetry of the temperature of the disk from a space experiment would then give not only the change in reflectivity of the disk but also, from correlation with the ground experiment, the micrometeoroid exposure causing this reflectivity change. The surface chosen for space-flight experiments, because of its initial fast rise in equilibrium temperature and large changes initially in  $\alpha_{sn}$  and  $\epsilon_{th}$  when exposed to simulated micrometeoroids, was the 1900 Å Al/stainless steel disk. Disks with 2000 Å of Al/stainless steel were placed thermally isolated from the spacecraft on OSO III and SERT II. The following section describes both of these space experiments and discusses the results.

### Space Experiments

#### SERT II—REX

The SERT II spacecraft was launched in 1970 as a 6-month test bed for the operation of an ion thruster in space.<sup>13</sup> A secondary experiment on the spacecraft, called REX (reflector

erosion experiment), was designed to measure micrometeoroid degradation of a highly reflective aluminum disk. This section presents the first published REX results. It covers space-obtained data from the first 9 months of the mission in 1970 and also data obtained during an extended mission through 1981, a total period of 11 years, 3 months in space.<sup>4,13</sup>

#### REX Description

Figure 5 shows an artist's drawing of the REX apparatus. Figure 5a is the mounting body used to control the thermal environment of the disk in the back hemisphere. Two disks, 2.38 cm in diameter and 0.013-cm thick, with a 2000 Å coating of aluminum vapor deposited on the disk front face, were used in this flight experiment. Figure 5b shows details of mounting the disk to the body. The mounting structure was designed to control heat transfer between the disk and body to a value between  $8.3$  to  $16.6 \times 10^{-18}$  W/K<sup>4</sup>. Cooldown data taken on the flight apparatus before launch determined the actual value to be  $13.3 \times 10^{-18}$  W/K<sup>4</sup>.

Thermistor sensors mounted on the two disk (disk no. 1 is the upper one, and disk no. 2 the lower) and on the front (semiside) plate of the body provided temperature data. The thermistor data were transferred via the connector plug (shown on the cup side) to the spacecraft telemetry system, which digitized it and radio-linked it to an Earth receiving station. Each digital bit was equivalent to 1 K, or the temperature step between measurable values. The thermistor sensors and

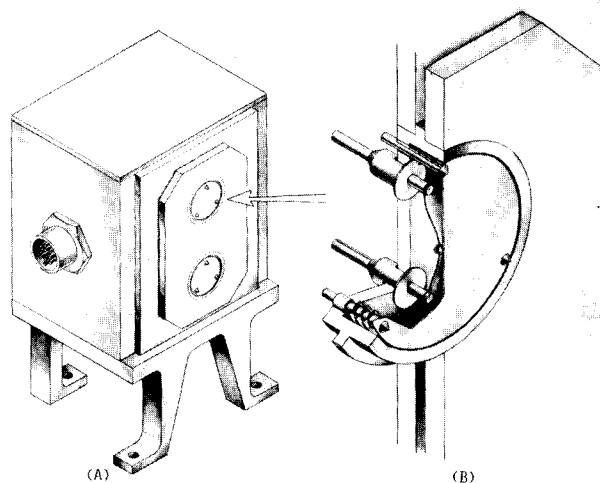


Fig. 5 Reflector erosion experiment, SERT II.

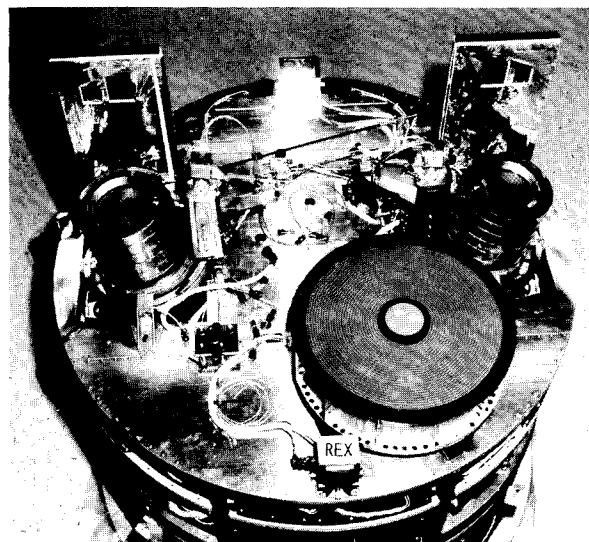


Fig. 6 Experiment deck of SERT II spacecraft.

telemetry system were calibrated before launch. The sensitivity of flight REX temperature data was  $\pm 0.5$  K. The sensor stability specification was  $\pm 0.5$  K for 6 months and is as good as the drift of the resistance of a high-quality resistor. The telemetry-thermistor ground calibration gave the absolute temperature to  $\pm 1$  K, and repeated in-space telemetry calibrations showed no discernable change in the telemetry system through 1981. The design range of the disk sensor was 325–380 K ( $T_1$  and  $T_2$ ), and the body sensor range was 266–349 K ( $T_b$ ). REX temperature sensors were scanned and recorded every 4 min by the telemetry system.

The REX body was mounted on the end deck of the SERT II spacecraft as shown in Fig. 6. A protective cover (removed before launch) was placed over the REX disks in Fig. 6. The disk front side (2000 Å aluminum) was in a plane perpendicular to the deck and had a nearly clear hemispherical view of space and Earth. The plane of the disk was in the spacecraft orbit plane. The launch time, direction, and altitude were picked to be sun-synchronous; thus, the orbit plane was nominally perpendicular to the sun direction ( $\theta_s = 0$  deg), and the REX disk surface was sun-facing. (The exact sun direction will be shown in the figures to follow.)

There was no direct line of sight between any active spacecraft component and the front disk surface. The mercury ion thruster exhaust consisted of 90% high-velocity (30,000 m/s), well-collimated ions, 9% neutral mercury atoms, and 1% low-velocity (1000 m/s) charge exchange ions. For any neutral exhaust atom to reach the disk front surface would require an improbable collision with a space particle downstream of the thruster exhaust, where the mean free path is greater than 1000 m. Because of the warm (340 K) disk temperature, any occasional mercury atom or ion arriving at the disk would re-evaporate. The ion thruster grids were made of molybdenum, and there was some ion sputtering of grid molybdenum.<sup>14</sup> If the molybdenum-sputtered atoms became charged, some would be attracted back to the spacecraft and, because of its low vapor pressure, would not re-evaporate. The most probable landing area would be on the deck or ion

thruster sides and not on the REX disks. Temperature sensors located on the deck, ion thruster side, and other thermal-emissive-sensitive places around the spacecraft<sup>6</sup> indicated no unexpected change in temperature during the mission. Perhaps the most sensitive sensor of all, the main solar arrays, showed less-than-predicted space degradation; thus, indications were that no molybdenum or any other condensable contaminant deposited on the REX disks.

#### REX Design Background

The REX experiment was designed to study the space temperature history of a highly reflective aluminum surface. The REX experiment was made  $\alpha_{sn}$ -change sensitive with small effects due to  $\epsilon_{th}$  changes. By using aluminum with an  $\alpha_{sn}$  of 0.111 and an  $\epsilon_{th}$  of 0.017, a heat transfer (disk-to-body) of  $13.3 \times 10^{-18}$  W/K<sup>4</sup>, and the micrometeoroid flux model of 1963<sup>2,3</sup> presented in Fig. 1, a REX disk temperature rise of 20–30 K was expected after 1 year in space. For example, the REX disk with a 0.22 J/cm<sup>2</sup> exposure of micrometeoroid flux would experience a 37 K temperature increase. This was the sum of a 42 K rise due to  $\alpha_{sn}$  increase and a 5 K drop due to  $\epsilon_{th}$  increase.

#### SERT II Spacecraft History

The SERT II spacecraft was launched in February 1970. Its major objective was the testing of an ion thruster in space for 6 months. A polar launch orbit was necessary to give a sun-synchronous orbit that would provide steady solar array power to operate the ion thrusters. The 1000-km orbit altitude was the highest available from the rocket launch vehicle. This was high enough to have a long decay orbit life (500 years) and have a low-density space background for ion thruster testing.

Because of a triaxial Earth, the orbit did not remain inertially fixed, but precessed slowly with a 20-year period. After 2 years, the orbit was no longer sun-synchronous (causing the spacecraft to enter the Earth's shadow), and the sun angle on the orbit plane (and solar array) changed from nearly normal to 31 deg off normal (upon first entering Earth's shadow). It then continued to 90 deg in 1975 and 180 deg in 1980.

To continue experiments past 1971, it was necessary to turn the solar array (and spacecraft) to face the sun to obtain enough power to operate experiments. To keep facing the sun, the spacecraft was spin-stabilized in 1973 (from 1970 to 1972, the spacecraft was gravity-gradient stabilized as shown in Fig. 7). Then, in late 1976, the original spin direction was changed to obtain more sun on the solar arrays and a proper orientation attitude for operation in 1979 when the orbit became sun-synchronous again. In late 1981, the orbit precession caused periods of Earth shadowing of the spacecraft, and spacecraft operations were terminated with the spacecraft in working order. Continuous sunlight orbit occurred again in 1989.

During the periods of Earth shadowing, the REX data were in nonthermal equilibrium, due not only to the shadow cooling, but also to large changes in sun angle caused by the spinning spacecraft. Therefore, no REX data are plotted for these periods. The precession or wobble of the spacecraft spin axis had a period of a few days to a few weeks. During the wobble periods, changes in REX disk temperature (293–320 K) were used to measure the wobble period and to calculate the sun angle on REX (and, hence, the main solar array). These calculations could be made because  $\alpha_{sn}$  and  $\epsilon_{th}$  had not changed significantly during the mission to that time.

During the spin-wobble years of 1973–1977, the REX disk was partially exposed to ram atomic oxygen. For those years, there was a period of 1145 days of such exposure. The ram angle on the disk varied from 0–18 deg (a perpendicular or direct ram angle would be 90 deg). Integration of the ram angles over the 1145 days resulted in an equivalent direct ram time of only 40.1 days. Because of the altitude (1000 km) and length of time in the ram direction, there is a negligible probability of atomic oxygen effects on the disks.

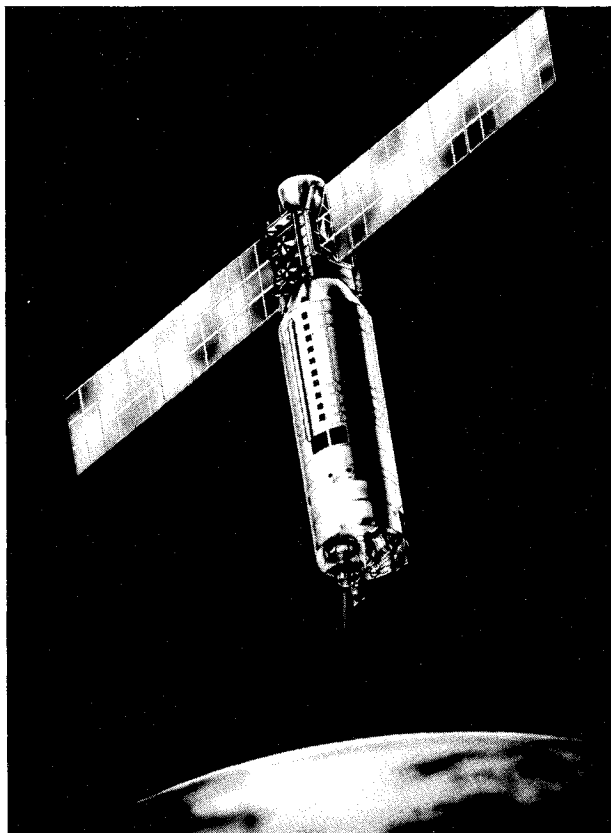


Fig. 7 SERT II spacecraft in orbit (artist's drawing).

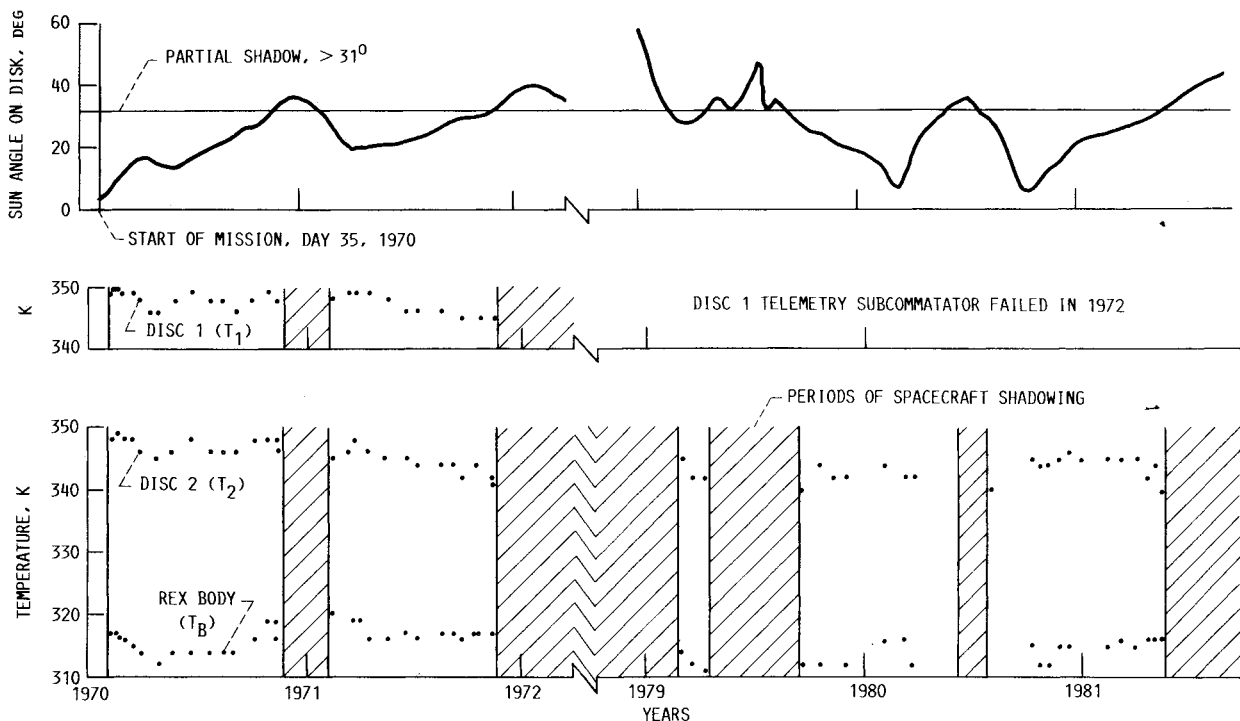


Fig. 8 Reflector erosion data (REX) taken on SERT II spacecraft.

#### REX Data

Figure 8 is a time plot of REX thermal data from launch (February 1970) to the end of data collection (May 1981). The two disk temperatures, the body or cup temperature, and sun angle of incidence on the disks were plotted. The shaded areas were times when the spacecraft was intermittently shadowed by the Earth. (See preceding SERT II Spacecraft History section.) All data on Fig. 8 were uncorrected. To minimize any variation due to Earth view factor or Earth albedo, only data taken when the spacecraft was over Fairbanks, Alaska, were plotted. This location was chosen because a majority of data came from the telemetry receiving station there. REX data were also compared over a ground station in Australia and showed no significant difference from the Alaska data.

The disk temperatures in Fig. 8 show almost no long-term change or trend with time. There seemed to be a small trend of lower disk temperature in the year 1971. The REX body or cup temperature was also fairly constant across time. The random, small temperature changes were partly due to changes of the sun angle causing local shadowing from the nearby RFI antenna (Fig. 6), sun rays reflecting off the aluminum spacecraft deck, or seasonal changes in Earth albedo. The change in sun angle closely followed the predicted orbit precession for the launch orbit. When the sun angle was larger than 31 deg, the spacecraft passed into the Earth's shadow, and no data were plotted due to nonnormal thermal equilibrium. Transient thermal data were not discriminant because the 4-min data sampling rate was large compared to the REX thermal time constant. Although no data were plotted for Earth shadow periods (i.e., 1972–1979), the REX disks were exposed to ambient micrometeoroid flux at all times. Temperature data from disk 1 were lost after 1972 when the telemetry subcommutator that processed disk 1 thermistor data stopped functioning.

#### REX Data Discussion

The disk temperature data of Fig. 8 can be enhanced by applying small corrections resulting from changes in REX body temperature and changes of incident solar intensity. Equation (B3) of Ref. 4 relates disk temperature ( $T_1$  or  $T_2$ ) with  $\alpha_{sn}$ ,  $\epsilon_{th}$ , REX body temperature, and solar intensity. A simplified form

of Eq. (B3) is presented below.

$$[T_1 \text{ or } T_2]^4 = \frac{[\alpha_{sn} + C_1 T_b^4 / \cos \theta_s]}{[C_2 \epsilon_{th} / \cos \theta_s + C_1 / \cos \theta_s]} \quad (5)$$

where  $C_1$  and  $C_2$  are constants.

For constant  $\alpha_{sn}$  and  $\epsilon_{th}$ , Eq. (5) reduces to the form

$$[T_1 \text{ or } T_2]^4 = C_3 \cos \theta_s + C_4 T_b^4 \quad (6)$$

where  $C_3$  and  $C_4$  are constants.

For the nominal values of  $\theta_s = 0$  deg and  $T_b = 316$  K,  $T_1$  or  $T_2 = 344$  K. Expected changes in  $T_1$  or  $T_2$  due to sun angle or body temperature changes can be calculated by using the actual instead of nominal values of  $\theta_s = 0$  and  $T_b = 316$  K. These calculated changes in  $T_1$  or  $T_2$  (amounting to  $-0.5$ – $8$  K) were used to correct or enhance the data of Fig. 8 by normalizing  $T_1$  or  $T_2$  to constant values of  $T_b$  and  $\theta_s$  (316 K and 0 deg). The corrected  $T_1$  and  $T_2$  data are plotted on Fig. 9.

Both the raw data (Fig. 8) and the normalized data (Fig. 9) showed the same major result. That is, there was no major change in disk temperature (a 30–40 K change was expected) due to exposure to space micrometeoroids over a period of 11 years and 3 months. This result indicated that the micrometeoroid flux model of the 1960's<sup>3</sup> (i.e., the 1963 model presented in Fig. 1) was considerably higher than the real flux.

#### OSO III

The 2000 Å Al/stainless steel reflector erosion micrometeoroid detector was also part of the thermal control coatings experiment flown on OSO III. This satellite was launched into a low-Earth, nearly circular equatorial orbit on March 8, 1967, and was operational for at least 5 years. The orbit altitude was about 550 km and was inclined 33 deg relative to the Earth's equator. The orbit period was 96 min, with about 60 min of the orbit being in sunlight. The satellite was spin-stabilized with a rate of 35 rpm. This spin axis was perpendicular to the satellite-sun line. Twelve coatings (mostly thermal control), mounted on thin disks about 1 in. (2.54 cm) in diameter, were exposed to the space environment; each



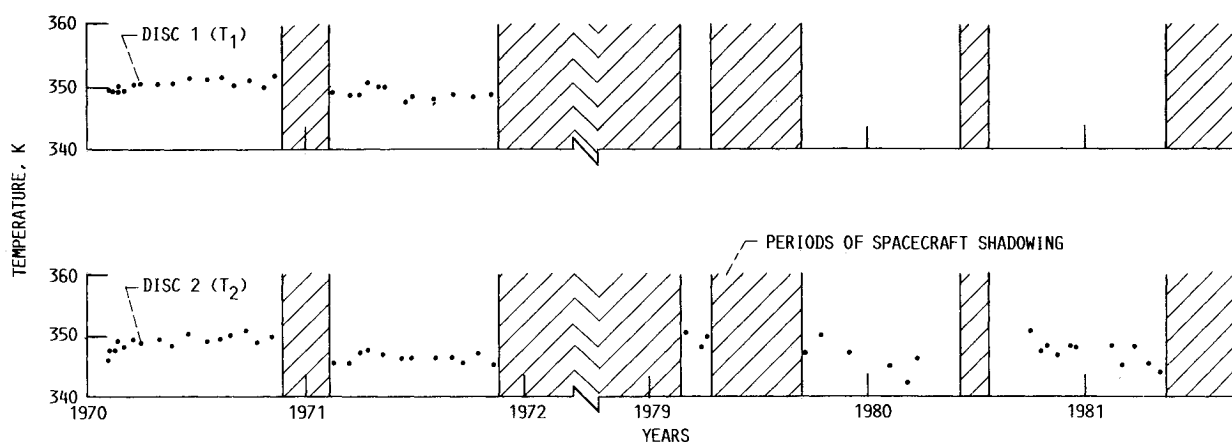


Fig. 9 Reflector erosion data (REX) normalized to constant REX body temperature (316 K) and constant sun incidence ( $\theta_s = 0$  deg).

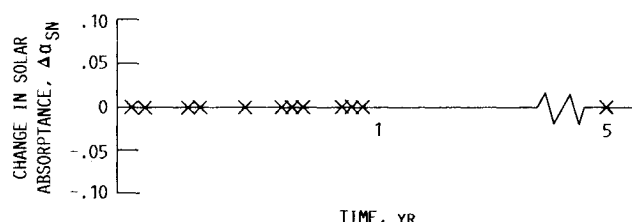


Fig. 10 Lack of change in solar absorptance of 2000 Å Al/stainless steel flown on OSO III.

coated disk was thermally isolated on the back side. Changes in solar absorptance  $\alpha_{sn}$  and thermal emittance  $\epsilon_{th}$  values were deduced from transient temperature measurements of the disks.

One of the results, written in 1968, and pointed out by the principal investigator,<sup>5</sup> was that for the 2000 Å Al on stainless steel, "No changes in  $\alpha_{sn}$  or  $\epsilon_{th}$  of the 2000 Å Al coating were detected in a time period of about 11 months. This result is highly significant in that it indicates effects of micrometeoroids were negligible."

Upon request, the transmitter was turned on and data obtained on the 2000 Å Al disk after 5 years in orbit. Again, there were no changes in  $\alpha_{sn}$  or  $\epsilon_{th}$  of the disk, indicating again that the effects of the micrometeoroid environment on this surface were negligible, even after 5 years in an equatorial orbit. These data are shown in Fig. 10 as  $\Delta\alpha_{sn}$  vs time. No change in  $\alpha_{sn}$  indicates no change in the total solar reflectance, since  $\rho_s = 1 - \alpha_{sn}$  for an opaque surface.

### Results and Discussion—Implication on Micrometeoroid and Space Debris Models and Erosion of Surface Optical Properties

As pointed out in the introduction, the placing of the micrometeoroid sensor (2000 Å Al/stainless steel) in space was founded on the 1963 interplanetary dust measurements presented in Fig. 1. From this model of the micrometeoroid environment, we expected a flux of approximately  $3.5 \times 10^5$  hits/cm<sup>2</sup> year, which is dominated by low-mass particles ( $10^{-12}$  to  $10^{-10}$  g). This translates to an energy flux on our sensor of approximately  $\frac{1}{3}$  J/yr ( $0.067$  J/cm<sup>2</sup> year) for a particle velocity of 20 km/s. The sensor sensitivity was, therefore, set for a minimum rise in temperature of 1 K because of this flux model. A simple calculation shows that the minimum energy that could be detected by the sensor, because of this sensitivity, was  $0.00067$  J/cm<sup>2</sup>. The REX disks on SERT II experienced no rise in temperature in 11 years and no change in solar absorptance in 5 years on OSO III. This certainly implies

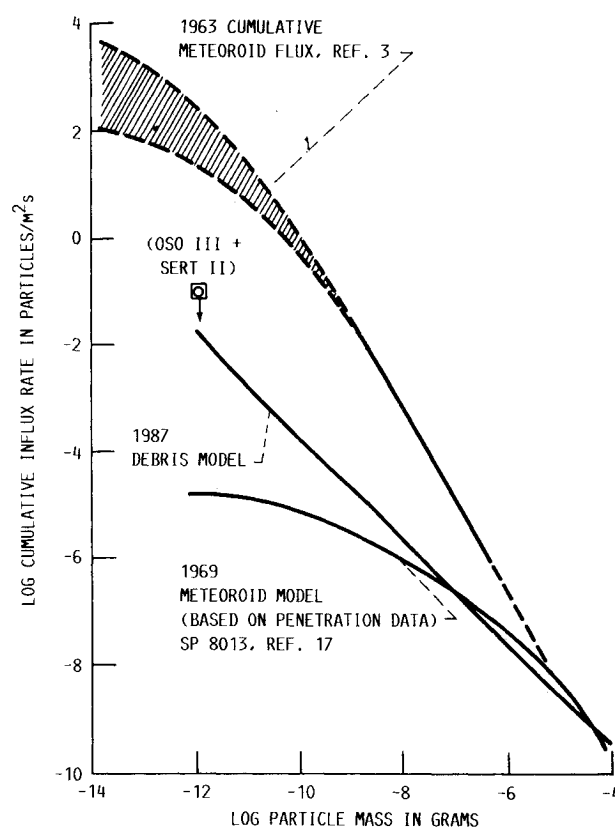


Fig. 11 Cumulative micrometeoroid and debris fluxes including the 1963 interplanetary dust measurements model, 1969 meteoroid model (based on penetration data only), 1987 debris model, and the OSO III and SERT II data.

that the energy of the impacting micrometeoroids was less than  $0.003$  J/11 years =  $0.00027$  J/yr or  $0.000067$  J/cm<sup>2</sup> year. Assigning a velocity of 20 km/s to the micrometeoroids yields a flux for the  $10^{-12}$ -g particles of approximately 350 hits/cm<sup>2</sup> year or  $10^{-1}$  hits/m<sup>2</sup> s, the minimum number of hits detectable by this sensor in 11 years.

These data are plotted on Fig. 11 along with the micrometeoroid flux models of Ref. 3 (1963), Ref. 17 (1969), and the 1987 space debris model presented by Jaffe.<sup>16</sup> The 1969 micrometeoroid flux model is based only on micrometeoroid penetration data. This NASA near-Earth micrometeoroid model has been widely accepted and continues to be used today even though it was first published in 1969. This is also cited by Jaffe<sup>16</sup> in an extensive review of available data on



the micrometeoroid and space debris environments. Jaffe cites and reviews 30 references in recommending models of these environments for the 100-kW space nuclear power system SP100.<sup>18</sup> In this reference, he discusses the studies of Kessler,<sup>19-22</sup> a debris model by Laurance and Brownlee<sup>23</sup> (based on pits on solar maximum surfaces), and meteoroid models generated by Aguero, McDonnell, Laurance and Brownlee, and Whipple<sup>16</sup> and Cour-Palais.<sup>17</sup>

The results of the SERT II or OSO III flight experiments are consistent with both the 1969 micrometeoroid and 1987 space debris flux models. In fact, they verify that the flux is less than or equal to the quantities observed, which is consistent with these models. This is why a vertical arrow is drawn down from the data point in Fig. 11, meaning that the flux was even less than our sensor could detect.

The resulting data imply that solar dynamic reflector surfaces such as the reflector surface (a highly polished metal or thin metal film deposit) flown in space should lose less than 1% of their specular reflectance over a period of 11 years. An extrapolation based on area damage derived from the 1987 micrometeoroid model and ground reduction in specular reflectance due to micrometeoroid simulation studies indicates that such a reduction in specular reflectance should not happen within the useful lifetime of currently conceived space systems.

### Concluding Remarks

A shock tube was used to accelerate micron-size particles to hypervelocities to simulate micrometeoroid impact on polished metal surfaces. An analytic expression was derived, which predicts reduction in reflectance of polished metal surfaces as a function of area damaged, that correlates with the kinetic energy of the impacting hypervelocity particles. A space simulation facility was used to calibrate a micrometeoroid sensor (2000 Å Al/stainless steel). It was found that this sensor, thermally isolated from the spacecraft, exhibited a rapid rise in equilibrium temperature when exposed to simulated micrometeoroid exposure. This micrometeoroid sensor was then flown on two satellites, OSO III (equatorial orbit) and SERT II (polar orbit). No changes in either equilibrium temperature or optical properties of the highly reflective surface were measured in 11 years in space. The effects of the space environment, i.e., the micrometeoroid environment on the solar reflectance, were negligible. The results are in agreement with the 1969 micrometeoroid flux model presented in the paper. From the accuracy of the sensor, the results indicate that a reflector surface (a highly polished metal or a thin metal film deposit) should lose less than 1% of its specular reflectance in near-Earth orbit in 11 years. This result alone will be very useful to the design of space solar dynamic/concentrator systems.

### References

- <sup>1</sup>Mirtich, M. J., and Mark, H., "Feasibility of Accelerating Micron-Size Particles in Shock-Tube Flow for Hypervelocity Degradation of Reflective Surfaces," NASA TN-D-3187, Jan. 1966.
- <sup>2</sup>Hawkins, G. S. (ed.), "Meteor Orbits and Dust," *Proceedings of a Symposium on Meteor Orbits and Dust*, Aug. 1965, NASA SP-135, SCA Vol. II, pp. 1-411.
- <sup>3</sup>Alexander, W. M., McCracken, C. W., Secretan, L., and Berg, O. E., "Review of Direct Measurements of Interplanetary Dust from

Satellites and Probes," *Proceedings of the Third International Space Sciences Symposium*, edited by W. Priester, J. Wiley, New York, 1963, Sec. C2, Paper 1, pp. 891-917.

<sup>4</sup>Mark, H., Sommers, R. D., and Mirtich, M. J., "Effect on Surface Thermal Properties of Calibrated Exposure to Micrometeoroid Environment," *AIAA Journal*, Vol. 4, No. 10, 1966, pp. 1811-1818.

<sup>5</sup>Millard, J. P., "Results from the Thermal Control Coatings Experiment on OSO-III," AIAA Paper 68-794, Jan. 1968.

<sup>6</sup>Parsons, R. L. and Gulino, D. A., "Effect of an Oxygen Plasma on Uncoated Thin Aluminum Reflective Films," NASA TM-89882, May 1987.

<sup>7</sup>Banks, B., Mirtich, M. J., Rutledge, S. K., and Swec, D. M., "Ion Beam Sputter Deposited Thin Film Coatings for Protection of Spacecraft Polymers in Low Earth Orbit," NASA TM-87051, Jan. 1985.

<sup>8</sup>Summers, R. D. and Mark, H., "Effect on Nonperfect Isolation in the Temperature of Metal Surfaces on Satellites," *AIAA Journal*, Vol. 4, No. 6, pp. 1092-1095.

<sup>9</sup>Mark, H., Goldberg, G., and Mirtich, M. J., "Determination of Cratering Energy Densities for Metal Targets by Means of Reflectivity Measurements," *AIAA Journal*, Vol. 2, No. 5, 1964, pp. 965-966.

<sup>10</sup>Summers, J. L., "Investigation of High-Speed Impact: Regions of Impact at Oblique Angles," NASA TN-D-94, 1959.

<sup>11</sup>Mirtich, M. J. and Mark, H., "Effect of Hypervelocity Projectile Material on the Ultimate Reflectance of Bombarded Polished Metals," NASA TM-X-52981, April 1971.

<sup>12</sup>Ugucini, O. W. and Pollack, J. L., "A Carbon-arc Solar Simulator," American Society of Mechanical Engineers, Pittsburgh, PA, Paper 62-WA-241, 1962.

<sup>13</sup>Kerslake, W. R., Goldman, R. G., and Wieberding, W. C., "SERT II Mission, Thrust Performance, and In-Flight Measurements," *Journal of Spacecraft and Rockets*, Vol. 8, March 1971.

<sup>14</sup>Kerslake, W. R., and Finke, R. C., "SERT II Spacecraft Thruster Restart 1974," *Journal of Spacecraft and Rockets*, Vol. 12, Dec. 1975.

<sup>15</sup>Mirtich, M. J. and Weigand, A. J., "Change in Transmittance of Fused Silica as a Means of Detecting Material Sputtered from Components in a 5-cm Ion Thruster," NASA TM-X-68073, May 1972.

<sup>16</sup>Jaffe, L., "Meteoroid and Debris Environment Models," Jet Propulsion Lab., Pasadena, CA, JPL-IOM 313/09, June 1987.

<sup>17</sup>Cour-Palais, B. G., "Meteoroid Environment Model," Near Earth to Lunar Surface, NASA SP-8013, 1969.

<sup>18</sup>Brandhorst, H. W., Jr., Juhasz, A. J., and Jones, B. I., "Alternative Power Generation Concepts for Space," NASA TM-88876, 1986.

<sup>19</sup>Kessler, D. J., "Orbital Debris Issues," *Space Debris, Asteroids and Satellite Orbits. Advances in Space Research*, Vol. 5, No. 2, 1985, pp. 3-10.

<sup>20</sup>Kessler, D. J., "Earth Orbital Pollution," *Beyond Spaceship Earth: Environmental Ethics and the Solar System*, edited by E. D. Hargrove, Sierra Book Club, San Francisco, CA, 1986, pp. 47-65.

<sup>21</sup>Kessler, D. J., "Sources of Orbital Debris and the Projected Environment for Future Spacecraft," *Journal of Spacecraft and Rockets*, Vol. 18, No. 4, 1981, pp. 357-380.

<sup>22</sup>Su, S. Y. and Kessler, D. J., "Contribution of Explosion and Future Collision Fragments to the Orbital Debris Environment," *Space Debris, Asteroids and Satellite Orbits: Advances in Space Research*, Vol. 5, No. 2, 1985, pp. 23-24.

<sup>23</sup>Laurance, M. R. and Brownlee, D. E., "The Flux of Meteoroids and Orbital Space Debris Striking Satellites in Low Earth Orbit," *Nature*, Vol. 323, 1986, pp. 136-138.